Kuwait J.Sci., Vol.49, No.(4),October.2022,pp(1-15)

Selective adsorption of cationic dye utilizing poly (methacrylic acid-co-ethylene dimethacrylate) monolith from wastewater

Bessy D'Cruz, Mohamed O. Amin, Metwally Madkour, Entesar Al-Hetlani*

Dept. of Chemistry, Faculty of Science, Kuwait University, P.O. Box 5969, Safat, 13060, Kuwait

**Corresponding author: entesar.alhetlani@ku.edu.kw*

Abstract

In this study, a poly (methacrylic acid-co-ethylene dimethacrylate (poly(MAA-co-EDMA)) monolith was prepared for the selective adsorption of acidic dye, namely, methylene blue (MB), from wastewater. The fabrication of the monolith was carried out via photoinitiation polymerization by irradiating a mixture of methacrylic acid (MAA), ethylene dimethacrylate (EDMA), porogenic solvents and an initiator. Batch adsorption assays were performed to examine the impact of monolithic dosage and initial dye concentration on the adsorption capacity and efficiency of the monolith towards MB dye molecules. This adsorption kinetic study revealed that MB adsorption on the monolith followed a pseudo-second-order model and equilibrium adsorption behavior was best modeled with the Langmuir adsorption isotherm, which indicated monolayer adsorption with a maximum adsorption capacity of 50.00 mg g^{-1}. Owing to the presence of negative binding sites on the monolithic surface, cationic MB molecules were selectively adsorbed in the MB/methyl orange (MO) mixture with an adsorption efficiency of 99.54% at equilibrium. Moreover, the MB-adsorbed monolith was regenerated up to four cycles, and the percentage removal efficiency of MB on the monolith dropped to 67.64 % after the fourth cycle. Finally, the monolith effectively adsorbed MB from the tap water in the presence of competing ions, and the maximum adsorptive capacity obtained was 47.62 mg g^{-1} with 84.5% adsorption efficiency. Hence, the poly(MAA-co-EDMA) monolith was found to be an adequate sorbent for the treatment of cationic dyes in the presence of other dyes and competing ions from wastewater.

Keywords: Acidic dye; adsorption; competitive sorption; methacrylate monoliths; wastewater

1. Introduction

Textile, leather, paper, plastic and other processing industries that utilize various dyes and pigments are major sources of water pollution. During the coloring process, it is estimated that 10-15% of the dyestuff is disposed into the aquatic environment; this is highly toxic and carcinogenic, even at trace-level concentrations. Dyes are highly colored and water-soluble materials; thus, they can reduce the amount of light penetrating the water. Subsequently, they have a derogatory impact on photosynthetic phenomena (B. Hameed & Ahmad, 2009). Therefore, dyes from wastewater should be removed or treated prior to their release into the environment to avoid serious health and environmental consequences (Parshetti, Parshetti, Kalyani, Doong & Govindwar, 2012).

Currently, several physical (D'Cruz, Madkour, Amin & Al-Hetlani, 2020), chemical (Al-Hetlani, Amin & Madkour, 2017) and biological (Bharti , 2019) approaches are employed to aid wastewater treatment. For example, coagulation/flocculation (Dotto, Fagundes-Klen, Veit, Palacio & Bergamasco, 2019), membrane filtration (Jiang *et al*., 2018), ozonation (Venkatesh, Venkatesh & Quaff, 2017) and biodegradation (B. B. Hameed & Ismail, 2018) are among the most commonly used methods in wastewater treatment. Although they are highly effective, they still suffer from some inherent limitations, e.g., some can be expensive and time consuming, require specialized equipment and generate secondary waste. Adsorption, in terms of promoting water purification, offers several advantages, such as the efficient adsorption of organic dyes using a variety of adsorbents organic, inorganic and hybrids (D'Cruz, Amin & Al-Hetlani, 2021; Thilagavathi, Arivoli & Vijayakumaran, 2015), and the ability to regenerate and reuse the adsorbents several times after the adsorption process (Astuti, Sulistyaningsih, Kusumastuti, Thomas & Kusnadi, 2019) using simple apparatuses. The level of adsorption efficiency is largely influenced by several factors, including the adsorbent properties and dosage as well as the adsorbate type, concentration and pH (Rajendran, Samuel, Amin, Al-Hetlani & Makhseed, 2020). Thus, it is imperative to optimize the experimental conditions to obtain a high adsorption efficiency.

A variety of organic, inorganic and hybrid adsorbents have been proposed for the adsorption of pollutants from wastewater. They display a range of properties, such as high porosity (Liu *et al*., 2021), hydrophobicity (Al-Hetlani, Amin, Bezzu & Carta, 2020), biocompatibility (Asadi, Eris & Azizian, 2018), surface chemistry (Islam *et al*., 2017) and others (Astuti *et al*., 2019), which can influence the adsorption process. Recently, organic polymers with controlled porosity, a large surface area and different functional groups have been the focus of many research studies (Shen *et al*., 2018). Such organic polymers have gained a lot of attention, and several organic polymers are already utilized as effective adsorbents to remove organic dyes from wastewater. For example, spirobifluorene polymers of intrinsic microporosity (PIMs) (Al-Hetlani, Amin, *et al*., 2020), porous organic polymers (POPs) (Al-Hetlani *et al*., 2021), hypercross linked porous polymers (Huang *et al*., 2018) and covalent organic frameworks (COFs) (Li, Yang, Qian, Zhao & Yan, 2019) have been successfully used for the adsorptive removal of organic dyes from wastewater. On one hand, despite their efficiency, the fabrication of these materials requires several steps and thorough purification of the final product. On the other hand, polymer monolithic materials (PMMs) are crosslinked co-polymers prepared via free-radical polymerization in a single step. They have been extensively utilized for chromatographic separation (F. Svec, E. C. Peters, D. Sýkora & J. M. J. Fréchet, 2000), solid-phase extraction (Fan, Feng, Zhang, Da & Zhang, 2005) and as solid supports for catalysis and other applications (Al-Hetlani, D'Cruz & Amin, 2020). PMMs are generated via thermal or photo-initiation in the presence of an initiator to generate free radicals, in the presence of a monomer to provide chemical functionality, a crosslinker to increase the mechanical strength of the polymer and porogenic solvents to control the porosity. They can be easily fabricated in large amounts (a few grams), and their functionality can be controlled with commercially available monomers; they have high pH stability, and most importantly, they are biocompatible (F. Svec, E. C. Peters, D. Sýkora & J. M. Fréchet, 2000).

In this work, we investigated the use of a poly (methacrylic acid-co-ethylenedimethacrylate) (poly(MAA-co-EDMA)) monolith for the adsorption of methylene blue (MB) dye from wastewater. To the best of our knowledge, these crosslinked co-polymers have not been previously employed for wastewater treatment applications. The polymer monolith was prepared using photo-initiation, and due to the abundance of the carboxylic acid groups in its skeleton which carry a negative charge, it was ideal for the selective adsorptive removal of cationic pollutants. The amount of poly(MAA-co-EDMA), the initial concentration of MB, the presence of competing ions from tap water, polymer selectivity towards anionic dye (methyl orange (MO) and reusability were investigated in this study.

2. Experimental

2.1 Materials and methods

Methacrylic acid (MAA), ethylene dimethacrylate (EDMA), 2,2-dimethoxy-2-phenylacetophenone (DAP), ethanol, toluene, 1-dodecanol, methylene blue (MB) and methyl orange (MO) were purchased from Sigma-Aldrich and were used as received. Throughout all experiments, double-distilled water was used.

2.2 Preparation of poly (MAA-co-EDMA) monolith

The fast and simple fabrication of methacrylic acid based monolith was adopted from (Al-Hetlani, D'Cruz, *et al*., 2020) and the pre-polymerization mixture was prepared by dissolving 0.237 mL of MAA, 1.998 mL of crosslinker EDMA and 0.023 g of initiator DAP in porogenic solvents, 1.45 mL of toluene and 4.35 mL of dodecanol. To obtain a homogeneous polymeric-mixture solution, this was sonicated for 20 minutes, followed by irradiation with a UV lamp (λ = 365 nm). To remove unreacted materials from the obtained polymer monolith, this was repeatedly washed with ethanol before being dried in an oven at 60 ºC overnight.

2.3 Adsorption of methylene blue from wastewater

The synthesized methacrylic acid based monolith was utilized in the adsorption batch assays. Variables affecting the monolithic absorption of MB, including the dose of the monolith, the initial dye concentration and contact time, were evaluated and optimized. All adsorption assays were conducted at room temperature using a 10 mL aqueous solution of MB and poly(MAA-co-EDMA) as the adsorbent, and the reaction mixture was sonicated for 20 min. Afterwards, the solution was filtered through a 0.45 µm GHP syringe filter to obtain clear filtrate; then, UV–Vis measurements at λ_{max} = 663 nm were performed to find the concentration of unadsorbed MB in the filtrate after adsorption. The percentage of dye removal (adsorption efficiency (%AE)) and the adsorption capacities of the adsorbent towards MB were calculated using the following equations:

$$\%AE = \frac{(C_o - C_t)}{C_o} \times 100 \quad (1)$$

$$q_{eq} = \frac{(C_0 - C_{eq})V}{m} \quad (2)$$

where C_o represents the initial MB concentration (mg L^{-1}); C_t and C_{eq} are the MB concentrations (mg L^{-1}) at time t and at equilibrium, respectively; V is the volume (L) of the MB solution; and m represents the mass of the adsorbent (g).

To investigate the adsorption selectivity of the monolith towards a mixture of organic dye molecules, 10 mg L^{-1} cationic MB and anionic MO mixture solution was chosen as the model initial concentration. The effectiveness of the monolith as an adsorbent for MB adsorption in tap water in the presence of competing ions was further examined with dye concentrations ranging from 10 to 50 mg L^{-1} under optimized adsorption conditions.

2.4 Regeneration of poly(MAA-co-EDMA)

To investigate the practical utility of the poly(MAA-co-EDMA) monolith as an adsorbent, adsorption–desorption experiments were conducted. The desorption experiment was studied with 25 mg of adsorbent and a constant initial MB concentration (10 mg L^{-1}) for a contact time of 20 min. The MB adsorbed monolith was collected via centrifugation, followed by washing five times with water and ethanol. Then, the adsorbent was dried at 80 ^{o}C overnight and reused for the next cycle. In this experiment, the adsorption–desorption cycle was repeated four times and the %AE was assessed in each cycle using equation.1.

3. Results and discussion

3.1 Adsorption experiments

The characterization of the fabricated monolith using several analytical techniques can be found in (Al-Hetlani, D'Cruz, *et al*., 2020). The maximum MB %AE with the minimum amount of monolith dose played a key role in wastewater treatment. Hence, the effect of the adsorbent dose towards the MB dye removal was investigated with various amounts of the monolith, ranging from 5 to 15 mg, mixed with the 10 mL MB solution (10 mg L^{-1}), and UV–Vis measurements were carried out. As depicted in Figure 1a, it was found that the adsorption efficiency increased from 97.81 to 99.71% with an increment in the adsorbent dose from 5 to 8 mg mL^{-1}; thereafter, a slight change in adsorption efficiency was observed. This could be attributed to the existence of a large number of adsorption binding sites for adsorbent–adsorbate interactions with the increase in the adsorbent dosage. However, the adsorption capacity showed a reverse trend with the further increase in adsorbent dosage. At higher monolith dosages, there is a higher chance for the collision and aggregation of poly(MAA-co-EDMA), which can limit the availability of binding sites for the adsorption process to proceed (D'Cruz *et al*., 2020). Therefore, 8 mg was chosen as the optimum adsorbent dosage to conduct the subsequent experiments.

In wastewater treatment, there is a direct relation between the adsorption efficiency and the initial MB concentration (Al-Ghouti & Al-Absi, 2020). Figure 1b shows the impact of the initial dye concentration on the %AE and the adsorption capacity of the monolith towards MB in the range from 5 to 50 mg L^{-1}. It was clear that, as the initial concentration of MB increased, the %AE increased up to 99.71% at 10 mg L^{-1}, and that at higher MB concentrations, the %AE decreased. However, the adsorption capacities of the monolith increased as the initial MB concentration increased. Due to this, the accessibility of the active sites on the poly(MAA-co-EDMA) monolith was high at the lower initial MB concentration, but the adsorption and mass transfer of MB were lowered at 5 mg L^{-1}, leading to a lower %AE. As the initial concentration of MB increased from 5 to 10 mg L^{-1}, the mass transfer resistance of dye molecules between water and adsorbent decreased, showing a higher %AE at 10 mg L^{-1}. Moreover, with the increase in the initial concentrations of MB above 10 mg L^{-1}, the saturation of the active adsorption sites on the adsorbent was observed, and consequently, the %AE decreased (Al-Ghouti & Al-Absi, 2020). Accordingly, 10 mg L^{-1} was selected as the initial concentration of MB for further studies.

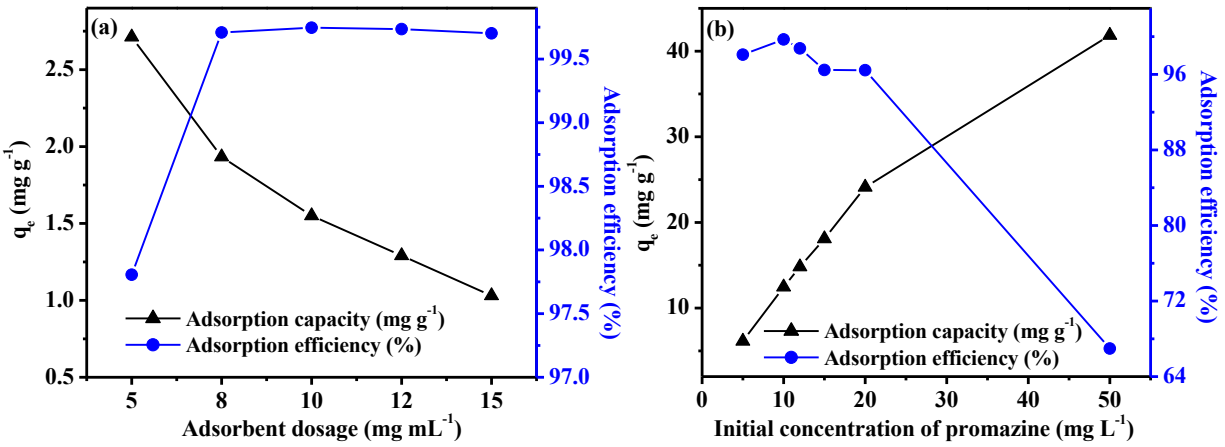

Fig. 1. Effects of (**a**) poly(MAA-co-EDMA) dosage (experimental conditions: C_0 = 10 mg L^{-1}; contact time = 20 min; total volume = 10 mL; 25 ºC) and (**b**) initial MB concentration (experimental conditions: adsorbent dosage = 8 mg; contact time = 20 min; total volume = 10 mL; 25 ºC) on adsorption efficiency and adsorption capacity.

3.2 Adsorption kinetics and isotherms studies

The effects of contact time between the monolith and dye molecules on the adsorption process were significant. Hence, the influence of contact time on the adsorption of MB onto the monolith was examined considering various time intervals under the optimum adsorption conditions, and the amount of MB adsorbed was calculated using equation 2. As depicted in Figure 2a**,** the adsorption capacity of the monolith was very high at the starting point of the adsorption process due to the presence of highly active vacant surface adsorption sites on the adsorbent, and with the increase in time, the saturation of the adsorption sites gradually occurred, followed by the state of

adsorption equilibrium, which was reached after 20 min. The amount of MB adsorbed, q_e, (exp, experimental) at equilibrium was found to be 12.47 mg g^{-1}.

In order to illustrate the adsorption mechanism behind MB adsorption onto the poly(MAA-co-EDMA) monolith, two conventional kinetic modelspseudo-first-order model and the pseudo-second-order model were employed (D'Cruz *et al.*, 2020). The suitability of the kinetic model was evaluated by comparing the correlation coefficients (R^2) or by comparing the amounts of MB adsorbed on the monolith estimated experimentally, q_e, (exp), and theoretically, q_e, (calc) (Sivaprakasam & Venugopal, 2019). The correlation coefficients (R^2) and q_e, (calc) obtained for the two models are reported in Table 1. It was clearly observed that the pseudo-second-order model was in good agreement with the experimental data calculated for the MB adsorption process on the binding sites of the monolith, as demonstrated in Figure 2b. Additionally, Langmuir and Freundlich models are well known to analyze the equilibrium adsorption isotherms data and simulate with the experimental data (D'Cruz *et al.*, 2020). Figure 3a illustrates the equilibrium adsorption of MB onto the poly(MAA-co-EDMA) monolith at different initial MB concentrations ranging from 10 to 50 mg L^{-1}**.** As can be seen, the adsorbent exhibited a maximum adsorption capacity of 50.00 mg g^{-1}. In addition, the equilibrium parameters of the isotherm models were calculated and are here listed in Table 1. The Langmuir adsorption isotherm model was better suited to describe the adsorption of MB on the active surface sites of the monolith, which could also be observed from the linear plot of the Langmuir adsorption isotherm displayed in Figure 3b. The Langmuir adsorption model assumes that the active adsorptive sites on the surface of a monolithic adsorbent are homogeneous in nature and that the adsorption process occurs uniformly within the adsorbent (monomolecular layer adsorption).

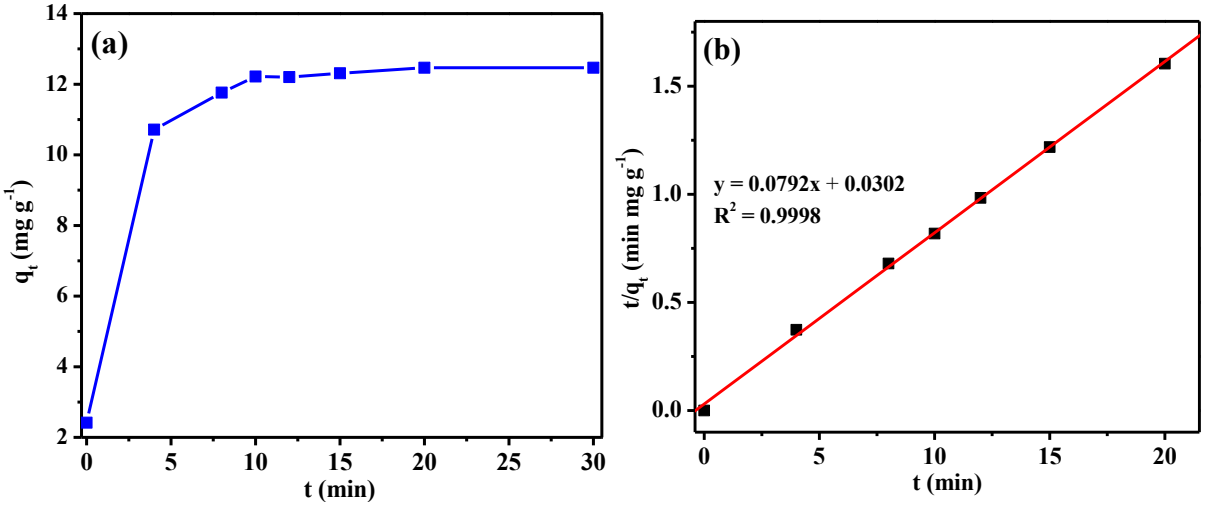

Fig. 2. (a) Influence of contact time on the adsorption capacity of poly(MAA-co-EDMA), towards MB. **(b)** Plot of pseudo-second-order kinetic model for the adsorption of MB onto poly(MAA-co-EDMA) (experimental conditions: initial concentration of MB = 10 mg L^{-1}; adsorbent dosage = 8 mg; 25 ºC).

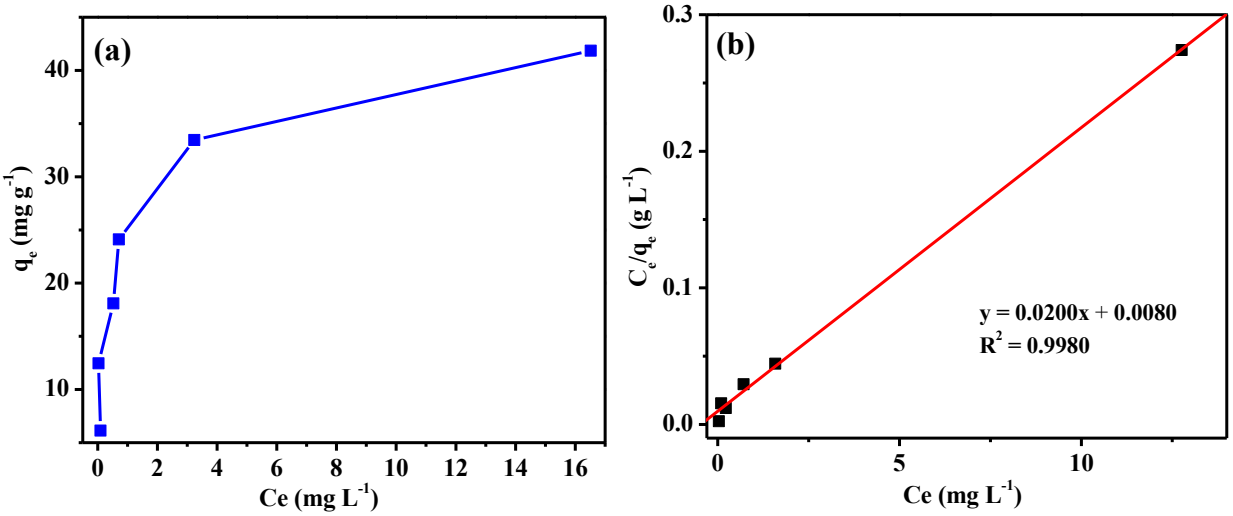

Fig. 3. (a) Adsorptionisotherm study of MB onto poly(MAA-co-EDMA). **(B)** Langmuir plot for MB adsorption onto poly(MAA-co-EDMA) (experimental conditions: adsorbent dosage = 8 mg; pH = 6.28; contact time = 20 min; 25ºC).

Table 1. Parameters of kinetic and isotherm adsorption models for MB adsorption onto the poly(MAA-co-EDMA) monolith.

Model	**Parameters**	**Values**
Pseudo-first-order model	k_1(min^{-1})	0.2780
	q_e (mg g^{-1})	6.90
	R^2	0.9450
Pseudo-second-order model	k_2(g mg^{-1} min^{-1})	0.2077
	q_e(mg g^{-1})	12.63
	R^2	0.9990
Langmuir isotherm model	K_L (L mg^{-1})	2.50
	q_m (mg g^{-1})	50.00
	R^2	0.9980
Freundlich isotherm model	K_F ((mg g^{-1}) (L mg^{-1})$^{1/n}$)	2.49 x 10^{-4}
	n	0.3962
	R^2	0.7360

The adsorption capacities towards MB of some adsorbents found in the literature are displayed in Table 2. Referring to the table, the adsorption capacity of poly(MAA-co-EDMA) towards MB was quite effective compared with other nanomaterials. This can be explained by the predominant negative charge on the surface of the polymer, which stimulated several electrostatic interactions between the adsorbent and the adsorbate (section 3.4).

Table 2. Adsorption capacity of other adsorbents for the removal of MB in aqueous solution.

Adsorbent	**Conditions**	**%Of removal**	**Adsorption capacity (mg g^{-1})**	**Reference**
$FeFe_2O_4$ magnetic nanomaterial	pH = 10; t = 80 min; C_0 = 100 ppm	35	42.35	(Dinh, Tran, Tran, & Nguyen, 2019)
Reduced graphene oxide	pH = 6.02; t = 30 min; C_0 = 100 ppm		121.95	(Arias Arias *et al*., 2020; Dinh *et al*., 2019)
Ag-Fe_3O_4-polydopamine	pH = 10; t = 26 hours	-	169.5	(Wu, Li, Yue, Zhang, & Huang, 2017)
Magnetic carboxyl functional nanoporous polymer	pH = 6.0; t = 30 min; C_0 = 15 ppm	90	57.74	(Su, Li, Han, & Liu, 2018)
g-C_3N_4 (Urea)	t = 50 min; C_0 = 0.5 ppm	-	2.51	(Zhu, Xia, Ho, & Yu, 2015)
CeO_2	pH = 9.0; MB t = 30 min; C_0 = 15 ppm	80.3	4.37	(Wei *et al*., 2019)
Poly(MAA-co-EDMA	pH = 6.28; contact time = 20 min; 25 ºC; C_0 = 10 ppm	99.54	50	This work

3. 3 Effect of water type

To examine the effect of competing ions on the adsorption capacity and %AE of the fabricated monolith for the removal of cationic dye MB from tap water, a series of adsorption experiments were conducted utilizing MB concentrations ranging from 10 to 50 mg L^{-1} with the optimum amount of adsorbent. Inductively coupled plasma mass spectrometry (ICP-MS) was used to examine the ions and their corresponding concentrations present in tap water, and $[Na^+]$ =13.90 mg L^{-1}, $[K^+]$ = 0.28 mg L^{-1}, $[Ca^{2+}]$ =21.62 mg L^{-1} and $[Mg^{2+}]$ = 1.85 mg L^{-1} were detected. The adsorption capacity and adsorption efficiency of the poly(MAA-co-EDMA) monolith towards MB

adsorption from tap water are shown in Figure 4. Indeed, no significant differences were evident in the %AE of the monolith when DI water was employed. The maximum adsorption capacity obtained was 47.62 mg g^{-1}, with 84.5% adsorption efficiency. It was found that the coexisting ions had an insignificant effect on the adsorption process of MB onto the poly(MAA-co-EDMA) monolith from tap water.

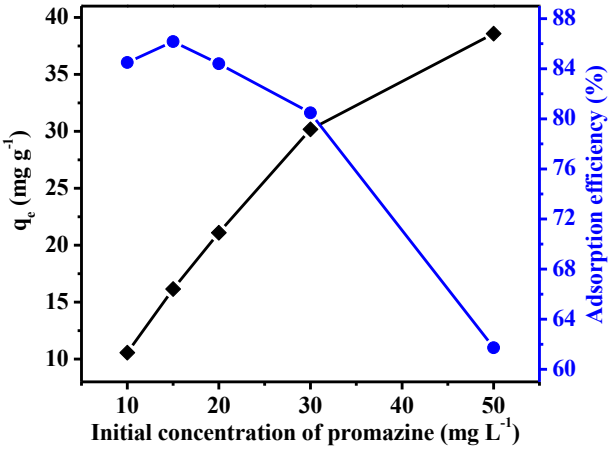

Fig. 4. Adsorption capacity and adsorption efficiency for the removal of MB from ordinary tap water samples using a poly(MAA-co-EDMA) monolith (experimental conditions: adsorbent dosage = 8 mg; initial concentrations of MB = 10-50 mg L^{-1}; contact time = 20 min; 25 ºC)

3.4 Selective adsorption and mechanism of MB from mixed dyes solution

To evaluate the selective adsorption property of the prepared monolith from a mixed dye solution, two kinds of dye molecules with different sizes and charges were used for the adsorption experiments (Pourzare, Farhadi, & Mansourpanah, 2018). Figure 5 presents the UV–Vis adsorption spectra for the adsorption of MB and MO from the MB/MO mixture onto the monolith under optimized conditions. The absorbance in the UV–Vis spectra of cationic MB declined within 25 min, indicating an enhanced adsorption property of the monolith towards MB dye molecules, while there was no adsorption of MO dye molecules from the mixture solution. The inset in Figure 5 represents photographs of the MB/MO mixture solution before and after the adsorption process that confirmed the presence of MO dye molecules after adsorption. Consequently, the adsorbent showed an excellent adsorption efficiency (99.54%) towards MB in the mixture after 20 min due to the surface charge property of the monolith. The measured initial solution pH of the MB/MO mixture was 6.28, and at this pH, the monolith possessed a negative zeta potential value of -17.10 mV (Al-Hetlani, D'Cruz, *et al*., 2020); hence, the surface of the monolith was eminently negatively charged. Consequently, the selective capture of positively charged MB in the MB/MO mixture was due to the electrostatic attraction between negatively charged carboxylate ligands on the surface of the monolith and positively charged MB dye molecules, as shown in Figure 6a. The stability of the monolith adsorbent before and after MB adsorption was investigated using scanning

electron microscopy with energy-dispersive X-ray spectrometry (SEM-EDX). Based on the micrographs shown in Figure 6b and c, no differences in the surface morphologies of the monolith before and after MB adsorption were evident**.** However, the elemental analysis of the monolith after MB adsorption confirmed the presence of nitrogen and sulfur in addition to carbon and oxygen, which indicated the successful adsorption of MB molecules on the monolith. Hence, poly(MAA-co-EDMA) is a promising adsorbent for the selective removal and separation of MB in wastewater treatment.

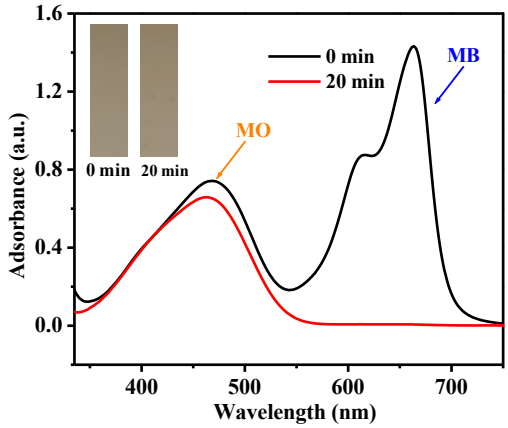

Fig. 5. UV–Vis adsorption spectra for the adsorption of MB and MO from the MB/MO mixture before and after adsorption onto the poly(MAA-co-EDMA) monolith (experimental conditions: adsorbent dosage = 8 mg; concentration of MB/MO mixture = 10 mg L^{-1}; pH = 6.28; contact time = 20 min). The corresponding photographs show the color change of the MB/MO mixture solution before and after adsorption.

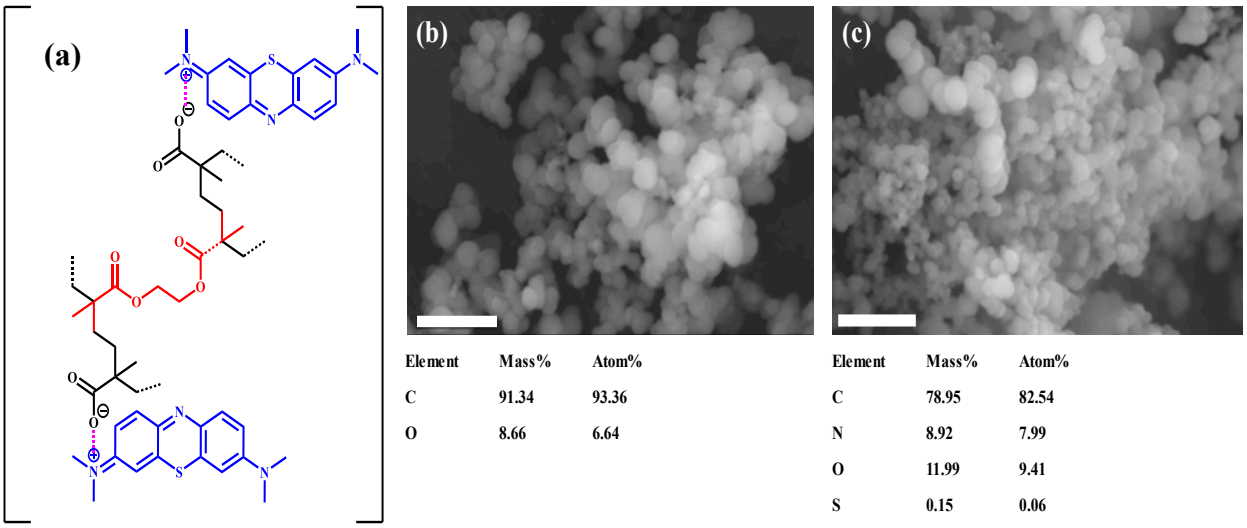

Fig. 6. (a) Adsorption mechanism of MB adsorption onto the poly(MAA-co-EDMA) monolith. **(b)** SEM-EDX analysis of the poly(MAA-co-EDMA) monolith before adsorption and **(c)** SEM-EDX analysis of the poly(MAA-co-EDMA) monolith after MB adsorption. Scale bar is 5 µm.

3.5. Desorption and reusability of poly(MAA-co-EDMA) monolith

The reusability of the used poly(MAA-co-EDMA) monolith was tested by performing four adsorption-desorption cycles of MB onto the adsorbent using ethanol and water as desorption eluents, and the results are shown in Figure 7. It was observed that the regenerated monolith could be used for two cycles without any remarkable decrease in the %AE, and after the sequence of two cycles, the %AE reduced from 97.97 to 77.13 %. Thus, the poly(MAA-co-EDMA) monolith could be employed for the removal of MB molecules from wastewater for up to four successive cycles.

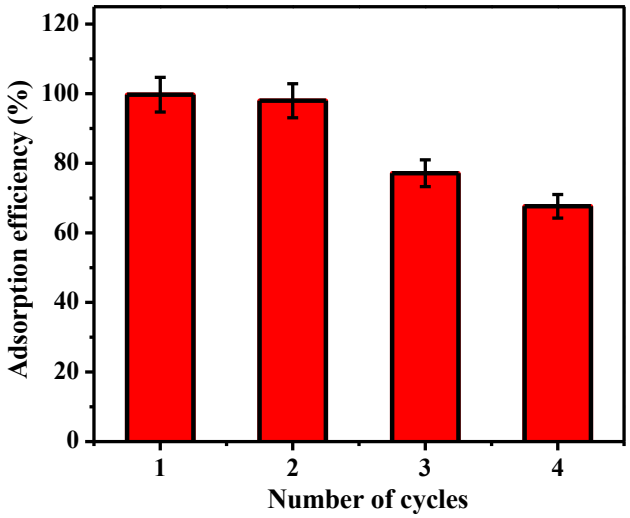

Fig. 7. The adsorption efficiency of the regenerated poly(MAA-co-EDMA) monolith for the removal of MB from wastewater after four adsorption-desorption cycles (conditions: initial MB concentration = 10 mg L^{-1}; adsorbent dosage = 8 mg; contact time = 20 min; 25 ºC).

4. Conclusion

For the first time, an organic-based monolith namely poly(MAA-co-EDMA) was employed for the selective adsorptive capture of MB from wastewater. The batch adsorption experiments were performed to examine the adsorption efficiency and capacity of the poly(MAA-co-EDMA) monolith, and under optimum conditions using 8 mg of the monolith and 10 mg mL^{-1} MB, the monolith exhibited an excellent adsorption efficiency of 99.71% towards MB. The kinetic adsorption model was described by the pseudo-second-order kinetic model, and the Langmuir adsorption isotherm described the equilibrium adsorption isotherm of MB adsorption over the monolith. Due to the high negative zeta potential of the monolith, the cationic dye molecules could rapidly and selectively adsorb onto the surface of the monolith via electrostatic attraction in aqueous solution in the presence of anionic MO dye. The adsorption process from the tap water confirmed that the poly(MAA-co-EDMA) monolith could be a potential adsorbent to selectively remove cationic dye molecules, which is very significant for environmental clean-up in the presence of competing ions. Finally, the monolith was successfully regenerated and reused for the removal of MB for four adsorption–desorption cycles.

ACKNOWLEDGMENTS

The authors gratefully acknowledge the Kuwait University research administration team and Kuwait Foundation for the Advancement of Sciences (KFAS grant no. P115-14SC-04). The authors would also like to offer their special thanks to KUNRF general facility No. GE 01/07 for zeta potential measurements and Mr. Hamidu B. Youngo for performing SEM and EDS analyses.

References

Al-Ghouti, Mohammad A. & Al-Absi, Rana S. (2020) Mechanistic understanding of the adsorption and thermodynamic aspects of cationic methylene blue dye onto cellulosic olive stones biomass from wastewater. Scientific Reports, 10(**1**), 1-18.

Al-Hetlani, Entesar, Amin, Mohamed O, Bezzu, C Grazia & Carta, Mariolino. (2020) Spirobifluorene-based polymers of intrinsic microporosity for the adsorption of methylene blue from wastewater: effect of surfactants. Royal Society open science, 7(**9**), 200741.

Al-Hetlani, Entesar, Amin, Mohamed O. & Madkour, Metwally. (2017) Detachable photocatalysts of anatase TiO2 nanoparticles: Annulling surface charge for immediate photocatalyst separation. Applied Surface Science, 411, 355-362.

Al-Hetlani, Entesar, D'Cruz, Bessy. & Amin, Mohamed O. (2020) A 3D miniaturized solid-state chemiluminescence sensor based on ruthenium functionalized polymeric monolith for the detection of pharmaceutical drugs. Journal of Materials Science, 55(**27**), 13232-13243.

Al-Hetlani, Entesar, Rajendran, Narendran, BabuVelappan, Anand, Amin, Mohamed O, Ghazal, Basma. & Makhseed, Saad. (2021) Design and Synthesis of a Nanopolymer for CO2 Capture and Wastewater Treatment. Industrial & Engineering Chemistry Research, 60, 8664−8676.

Arias Arias, Fabian, Guevara, Marco, Tene, Talia, Angamarca, Paola, Molina, Raul, Valarezo, Andrea, . . . Caputi, Lorenzo S. (2020) The adsorption of methylene blue on eco-friendly reduced graphene oxide. Nanomaterials, 10(**4**), 681.

Asadi, Safoura, Eris, Setareh & Azizian, Saeid. (2018) Alginate-Based Hydrogel Beads as a Biocompatible and Efficient Adsorbent for Dye Removal from Aqueous Solutions. ACS Omega, 3(**11**), 15140-15148.

Astuti, Widi, Sulistyaningsih, Triastuti, Kusumastuti, Ella, Thomas, Gui Yanny Ratna Sari & Kusnadi, Rizky Yogaswara. (2019) Thermal conversion of pineapple crown leaf waste to magnetized activated carbon for dye removal. Bioresource technology, 287, 121426.

Bharti, Vikash, Vikrant, Kumar, Goswami, Mandavi, Tiwari, Himanshu, Sonwani, Ravi Kumar, Lee, Jechan, . . . Kumar, Sunil. (2019) Biodegradation of methylene blue dye in a batch and continuous mode using biochar as packing media. Environmental research, 171, 356-364.

D'Cruz, Bessy, Madkour, Metwally, Amin, Mohamed O. & Al-Hetlani, Entesar. (2020) Efficient and recoverable magnetic AC-Fe3O4 nanocomposite for rapid removal of promazine from wastewater. Materials Chemistry and Physics, 240, 122109.

D'Cruz, Bessy, Amin, Mohamed O. & Al-Hetlani, Entesar. (2021) Polyoxometalate-Based Materials for the Removal of Contaminants from Wastewater: A Review. Industrial & Engineering Chemistry Research, 60(**30**), 10960-10977.

Dinh, Van-Phuc, Tran, Ngoc Quyen, Tran, Quang-Huy. & Nguyen, Trinh Duy. (2019) Facile synthesis of FeFe2O4 magnetic nanomaterial for removing methylene blue from aqueous solution. Progress in Natural Science: Materials International, 29(**6**), 648-654.

Dotto, Juliana, Fagundes-Klen, Marcia Regina, Veit, Marcia Teresinha, Palacio, Soraya Moreno. & Bergamasco, Rosangela. (2019) Performance of different coagulants in the coagulation/flocculation process of textile wastewater. Journal of Cleaner Production, 208, 656-665.

Fan, Yi, Feng, Yu-Qi, Zhang, Jian-Tao, Da, Shi-Lu. & Zhang, Min. (2005) Poly (methacrylic acid-ethylene glycol dimethacrylate) monolith in-tube solid phase microextraction coupled to high performance liquid chromatography and analysis of amphetamines in urine samples. Journal of Chromatography A, 1074(**1-2**), 9-16.

Hameed, Basma B. & Ismail, Zainab Z. (2018) Decolorization, biodegradation and detoxification of reactive red azo dye using non-adapted immobilized mixed cells. Biochemical Engineering Journal, 137, 71-77.

Hameed, BH. & Ahmad, AA. (2009) Batch adsorption of methylene blue from aqueous solution by garlic peel, an agricultural waste biomass. Journal of hazardous materials, 164(**2-3**), 870-875.

Huang, Yipeng, Ruan, Guihua, Ruan, Yuji, Zhang, Wenjuan, Li, Xianxian, Du, Fuyou, . . . Li, Jianping. (2018) Hypercrosslinked porous polymers hybridized with graphene oxide for water treatment: dye adsorption and degradation. RSC advances, 8(**24**), 13417-13422.

Islam, Md Tariqul, Hernandez, Cesar, Ahsan, Md Ariful, Pardo, Andrew, Wang, Huiyao & Noveron, Juan C. (2017) Sulfonated resorcinol-formaldehyde microspheres as high-capacity regenerable adsorbent for the removal of organic dyes from water. Journal of environmental chemical engineering, 5(**5**), 5270-5279.

Jiang, Mei, Ye, Kunfeng, Lin, Jiuyang, Zhang, Xinying, Ye, Wenyuan, Zhao, Shuaifei, & Van der Bruggen, Bart. (2018) Effective dye purification using tight ceramic ultrafiltration membrane. Journal of Membrane Science, **566**, 151-160.

Li, Yang, Yang, Cheng-Xiong, Qian, Hai-Long, Zhao, Xu & Yan, Xiu-Ping. (2019) Carboxyl-Functionalized Covalent Organic Frameworks for the Adsorption and Removal of Triphenylmethane Dyes. ACS Applied Nano Materials, 2(**11**), 7290-7298.

Liu, Xiaolu, Pang, Hongwei, Liu, Xuewei, Li, Qian, Zhang, Ning, Mao, Liang, . . . Wang, Xiangke. (2021) Orderly Porous Covalent Organic Frameworks-based Materials: Superior Adsorbents for Pollutants Removal from Aqueous Solutions. The Innovation, 2(**1**), 100076.

Parshetti, Ganesh Kashinath, Parshetti, Supriya, Kalyani, Dayanand C, Doong, Ruey-an & Govindwar, Sanjay P. (2012) Industrial dye decolorizing lignin peroxidase from Kocuria rosea MTCC 1532. Annals of microbiology, 62(**1**), 217-223.

Pourzare, Kolsoum, Farhadi, Saeed & Mansourpanah, Yaghoub. (2018) Anchoring H3PW12O40 on aminopropylsilanized spinel-type cobalt oxide (Co3O4-SiPrNH2/H3PW12O40): A novel nanohybrid adsorbent for removing cationic organic dye pollutants from aqueous solutions. Applied Organometallic Chemistry, 32(**5**), e4341.

Rajendran, Narendran, Samuel, Jacob, Amin, Mohamed O, Al-Hetlani, Entesar & Makhseed, Saad. (2020) Carbazole-tagged pyridinic microporous network polymer for CO2 storage and organic dye removal from aqueous solution. Environmental research, 182, 109001.

Shen, Xiaochen, Ma, Si, Xia, Hong, Shi, Zhan, Mu, Ying & Liu, Xiaoming. (2018) Cationic porous organic polymers as an excellent platform for highly efficient removal of pollutants from water. Journal of Materials Chemistry A, 6(**42**), 20653-20658.

Sivaprakasam, A & Venugopal, T. (2019) Modelling the removal of lead from synthetic contaminated water by activated carbon from biomass of Diplocyclos Palmatus by RSM. Global Nest Journal, 21(**3**), 319-327.

Su, Hongxin, Li, Weiwei, Han, Yide & Liu, Ningning. (2018) Magnetic carboxyl functional nanoporous polymer: synthesis, characterization and its application for methylene blue adsorption. Scientific Reports, 8(**1**), 1-8.

Svec, Frantisek, Peters, Eric C, Sýkora, David, & Fréchet, Jean MJ. (2000) Design of the monolithic polymers used in capillary electrochromatography columns. **Journal of Chromatography A,** 887(**1-2**), 3-29.

Svec, Frantisek, Peters, Eric C., Sýkora, David, & Fréchet, Jean M. J. (2000) Design of the monolithic polymers used in capillary electrochromatography columns. Journal of Chromatography A, 887(**1**), 3-29.

Thilagavathi, Muthaiyan, Arivoli, Shanmugam, & Vijayakumaran, Vaithilingam. (2015) Adsorption of malachite green from waste water using prosopis juliflora bark carbon. Kuwait Journal of Science, 42(**3**) 120-133.

Venkatesh, Smita, Venkatesh, Kumar, & Quaff, Abdur Rahman. (2017) Dye decomposition by combined ozonation and anaerobic treatment: Cost effective technology. Journal of applied research and technology, 15(**4**), 340-345.

Wei, Xiaoshu, Wang, Yi, Feng, Yuqian, Xie, Xiaomin, Li, Xiaofeng, & Yang, Sen. (2019) Different adsorption-degradation behavior of methylene blue and Congo red in nanoceria/H 2 O 2 system under alkaline conditions. Scientific Reports, 9(**1**), 1-10.

Wu, Maoling, Li, Yinying, Yue, Rui, Zhang, Xiaodan, & Huang, Yuming. (2017) Removal of silver nanoparticles by mussel-inspired Fe 3 O 4@ polydopamine core-shell microspheres and its use as efficient catalyst for methylene blue reduction. Scientific Reports, 7(**1**), 1-9.

Zhu, Bicheng, Xia, Pengfei, Ho, Wingkei, & Yu, Jiaguo. (2015) Isoelectric point and adsorption activity of porous g-C3N4. Applied Surface Science, 344, 188-195.

Submitted: 12/08/2021
Revised: 31/10/2021
Accepted: 03/11/2021
DOI: 10.48129/kjs.15647